Chinese Chemical Letters 34 (2023) 107963

Contents lists available at ScienceDirect

Chinese Chemical Letters

journal homepage: www.elsevier.com/locate/cclet

Effects of trifluoromethanesulfonic acid ligand on the Zinc-based catalysts for the acetylene hydration

Zhen Chen[a], Fei Zhao[b,c], Houyu Zhang[b], Qinqin Wang[a,*], Bin Dai[a,*]

[a] School of Chemistry and Chemical Engineering, Shihezi University/State Key Laboratory Incubation Base for Green Processing of Chemical Engineering, Shihezi 832000, China
[b] State Key Laboratory of Supramolecular Structure and Materials, Institute of Theoretical Chemistry, College of Chemistry, Jilin University, Changchun 130012, China
[c] School of Chemistry and Chemical Engineering, Taishan University, Tai'an 271000, China

ARTICLE INFO

Article history:
Received 8 August 2022
Revised 12 October 2022
Accepted 27 October 2022
Available online 30 October 2022

Keywords:
Acetylene hydration
Acetaldehyde
Zn-ligand catalysts
XAFS
DFT computation

ABSTRACT

Developing an efficient Zn-based catalyst modified with Trifluoromethanesulfonic acid (TfOH) ligand is extremely desirable for the acetylene hydration reaction. In this paper, with the use of a simple impregnation method, a series of Zn-TfOH/AC catalysts were synthesized, and the Zn-1.5TfOH/AC catalyst demonstrated the optimal catalytic performance with 96% acetylene conversion in the hydration of acetylene. The X-ray absorption fine structure (XAFS) spectra of the fresh Zn-1.5TfOH/AC catalysts demonstrated the establishment of the Zn-O4 coordination structure. According to the characterization results, TfOH ligands effectively inhibited carbon accumulation and Zinc loss, improved acidic sites and the dispersion of active metal, and produced more catalytic active site. Furthermore, the hydration reaction mechanism of Zn-TfOH/AC catalyst with $Zn(OTf)_2$, TfO-ZnCl, and TfO-ZnOH complex configurations was explored by the Density Functional Theory (DFT) method, which showed that the activation barrier increased sequentially TfO-ZnOH < $Zn(OTf)_2$ < TfO-ZnCl. Importantly, the OH^- in TfO-ZnOH is involved in the reaction and regenerated by the dissociation of H_2O, which lowers the energy barrier. This will provide a reference to design more efficient nonmercury catalysts for acetylene hydration.

Acetaldehyde, an intermediate of extremely important industrial chemicals, has a wide range of applications in pharmaceuticals, food and feed additives [1]. With the continued development of industry, the global demand for acetaldehyde would continue to increase in the future [2]. Acetaldehyde has been primarily generated by the ethylene and acetylene processes [3–5]. However, for the countries with abundant coal supplies, the acetylene process pathway for acetaldehyde production would be still of high research value [6], such as China. Currently, metals such as Hg [7–9], Cd [10,11], Au [12,13], Ru [14,15], Cu [16], and Zn [17] have been developed for alkyne hydration. Due to the Au and Ru metals are relatively expensive, reactive metal Cu ions are readily reduced to copper monomers, and Cd and Hg toxic metals [18]. Thus, the low price and high initial performance of active Zn-based catalysts would be more suitable for acetylene hydration reaction. However, the shortcomings of Zn-based catalysts, such as poor catalytic performance and stability, could not allow ignoring. Therefore, there is an urgent need to develop simple and efficient Zn-based catalysts for acetylene hydration reactions.

At present, the studies mainly focused on the carrier and active ingredients modification. Wang *et al.* [19,20] found that the use of amino (APTES, PEI) modified mesoporous MCM-41 carriers could effectively improve the catalyst dispersion and enhance the metal-carrier force to increase the electron cloud density around the active Zn ingredient, thereby improving the catalytic performance of Zn-based catalysts. Subsequently, research of Zr-modified ZSM-5 zeolites revealed that increasing concentrations of weak acid sites and active sites boosted hydration catalytic activity, with more than 96% acetylene conversion [21]. Wang *et al.* [22] investigated bimetallic catalysts and found that the synergistic effect of Cu and Zn was able to inhibit Zinc species loss, resulting in an acetylene conversion rate of up to 98%. Furthermore, they attempted to impregnate Zn onto Ti-doped MCM-41 carriers, which effectively boosted particle size control and hindered carbon deposition [23]. The results showed that after 10 h, the selectivity of acetylene reached 90%. Li *et al.* [24] systematically investigated the mechanisms of such reactions on $ZnCl_2$, Zn(OH)Cl, and $Zn(OH)_2$ catalysts through density functional theory (DFT) methods. They

* Corresponding authors.
E-mail addresses: wqq_shzu@sina.com (Q. Wang), db_tea@shzu.edu.cn (B. Dai).

https://doi.org/10.1016/j.cclet.2022.107963
1001-8417/

found that the energy required for breaking the O – H bond in water determined the activation energy of catalytic processes. Then, they reported a single-atom catalyst (ZnN_4S_2-SAC) with S and N co-doped defective graphene carriers, which modified the electronic structure of acetylene upon adsorption and facilitated the hydration reaction [25]. Yang *et al.* [26] investigated the performance of S-containing ligands on copper-based catalysts in acetylene hydration processes and deduced the catalytic reaction mechanism in conjunction with DFT calculations. Zhang *et al.* [27] introduced HEDP ligands by impregnation, which successfully blocked the reduction of Cu ions during the acetylene hydration processes. Furthermore, the synergistic interaction between ionic liquids (IL) and Cu species inhibited the loss of Cu while enhancing Cu species dispersion [28]. At $GHSV_{C_2H_2} = 90\ h^{-1}$ and $V_{H_2O}/V_{C_2H_2} = 1.15$, acetaldehyde selectivity was greater than 90%. Liu *et al.* [29]. Synthesized N and P co-doped Cu-based catalysts, which significantly increased the dispersion of the active component Cu, while inhibiting the reduction of high-valent Cu. The acetylene conversion reached 90% when the N and P doping concentrations were 0.40% and 2.61%, respectively.

Although substantial progress has been made in zinc and copper-based catalysts, there are still flaws that cannot be ignored. To begin with, MCM-41 molecular sieve is expensive and has poor hydrothermal stability. Second, in the study of transition metal modified carriers, the doping amounts of transition metals Zr and Ti are excessively high. Furthermore, the relevant papers for Cu-based catalysts have not yet confirmed whether the active species is Cu^{2+} or Cu^{+}, and there is no specific study on the reaction mechanism.

In recent years, ligand catalysts have been widely used in various catalytic reactions, which can help to modulate the catalytic site environment and enhance the catalytic activity. Liu *et al.* [30] explored the mechanism of $[W^{IV}O(mnt)_2]^{2-}$ on acetylene hydration in conjunction with DFT, hypothesizing that an OH^- containing model may be the reaction mechanism for catalytic acetylene hydration. Najafian *et al.* [31] combined DFT calculations and natural bond orbital theory to investigate the effect of different metal and ligand substituents on the catalytic properties of acetylene hydration, which found that electron-absorbing substituents significantly reduced the activation free energy and that less polar active sites were more favorable for acetylene hydration. Trifluoromethanesulfonic acid (TfOH), a strong organic Lewis acid that has been employed as a ligand for several transition metals in a range of acid-catalyzed processes due to its great thermodynamic stability and strong proton giving ability. Mugio *et al.* [32] found that $Hg(OTf)_2$ has significant catalytic activity to obtain methyl ketones with high catalytic turnover by achieving the hydration of terminal alkynes. R. E. Ebule *et al.* [33] investigated the effect of TfOH ligands on Au-catalyzed liquid-phase alkyne hydration processes, achieving complete conversion at low gold catalyst loading (0.01%) at room temperature. Bai *et al.* [34] revealed the mechanism of Janus polymerization in conjunction with DFT and found that the rare earth element Sc can form a five-ligand structure with the O atom in TfOH. The preceding research demonstrates that TfOH can be used as a ligand for several transition metals in a wide range of catalytic processes. Therefore, it is also worthwhile to investigate the performance enhancement of acetylene hydration process by zinc ligand catalysts.

In this work, a series of Zn-TfOH/AC catalysts were synthesized by impregnation method as effective catalysts for acetylene hydration. The aim of this study was to investigate the effect of TfOH ligands on the activity of Zn catalysts in acetylene hydration and whether the introduction of TfOH ligands helps to modulate the catalytic environment of Zn catalysts. Then, on the basis of the activity test and characterization results, the reasons for the promotion of activity are presented and discussed in detail. Finally, the potential ligand structure and its reaction mechanism are inferred by combining DFT calculations. The development of more effective zinc-based catalysts in terms of thorough investigation of the reaction mechanism is critical in the industrial application of acetylene hydration.

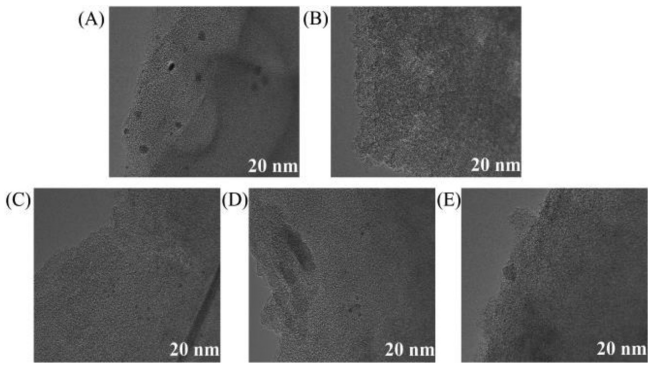

Fig. 1. TEM images of fresh catalysts: Zn/AC (A), Zn-0.5TfOH/AC (B), Zn-TfOH/AC (C), Zn-1.5TfOH/AC (D), Zn-2TfOH/AC (E).

In this experiment, the raw materials, catalyst preparation methods, characterization instrument information, performance evaluation methods, and DFT methods used were shown in the Supporting information.

According to the physical structures and N_2 adsorption desorption isotherms of all catalysts shown in Table S1 and Fig. S1 (Supporting information), the pore volume and specific surface area of the catalysts decreased significantly after the addition of TfOH, which may be due to the fact that Zn-TfOH complex occupied the pore channel. It can be seen from the TG curve of fresh catalysts in N_2 atmosphere in Fig. S2 (Supporting information) that the ligand catalyst has good thermal stability and will not decompose at 240 °C. The FT-IR spectrum of the fresh catalyst in Fig. S3 (Supporting information) indicates that the TfOH ligand has been successfully bound to the surface of the carbon support.

To explore the dispersion of Zinc species in fresh catalysts from a microscopic perspective, fresh catalysts samples were analyzed by TEM and the results are shown in Fig. 1. Fresh Zn-based catalysts showed substantial agglomeration, whereas agglomeration was significantly decreased in catalysts after ligand addition. The results indicated that TfOH ligands could significantly promote the dispersion of active ingredients and inhibit the agglomeration of Zinc species during catalyst preparation, which could have a positive effect on the catalytic performance of acetylene hydration.

The acidity of catalysts has a great influence on their catalytic performance. Hence, to further investigate the variation of acid point type and acid concentration of the catalysts, Py-FTIR spectroscopy was performed on fresh catalysts, and the results are shown in Fig. 2 and Table S2 (Supporting information). According to the literature, the 1450 cm^{-1} peak represents the Lewis acid site, the 1540 cm^{-1} peak represents the Bronsted acid site, and the 1490 cm^{-1} absorption peak indicates both the Lewis and Bronsted acid sites [35,36]. The three peaks of the catalyst at 1446 cm^{-1}, 1492 cm^{-1}, 1548 cm^{-1}, and 1610 cm^{-1} correspond to the L acid sites, L + B acid sites, B acid sites, and strong acid sites, respectively, as illustrated in Fig. 2.

To investigate the chemical state and coordination environment of Zn in fresh Zn-1.5TfOH/AC catalyst, it was further characterized by synchrotron radiation in conjunction with XANES and EXAFS of the zinc K-edge. As shown in Fig. S4 (Supporting information), only the ZnO and Zn wavelets are found in the sample obviously only has one atomic signal. This is the Zn–O signal, which can be analyzed from the contour center coordinates in the wavelet, the sam-

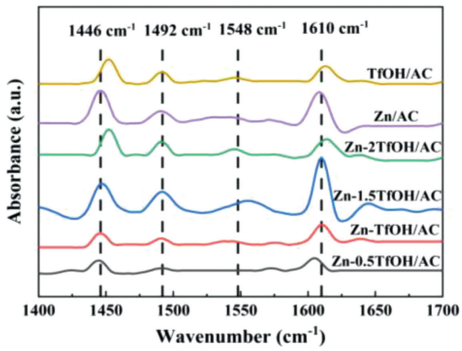

Fig. 2. Py-FTIR spectrum of fresh catalysts.

ple ZnO signal, and the Zn−O in ZnO specifically, the *k* value in the sample is slightly larger than ZnO, and the *R* value is also larger than ZnO, confirming the EXAFS data and the fitted structural parameters in Table S3 (Supporting information).

The X-ray absorption near-side structure spectrum of the fresh Zn-1.5TfOH/AC catalyst is shown in Fig. S5 (Supporting information). The intensity of the white line for Zn-1.5TfOH/AC is higher than the reference value for Zn metal, as shown in Fig. S5A, and the leading-edge transfers to higher energies, also close to the white line for ZnO. The absorption edge motion indicates that Zn is in the oxidation state, and the sample absorption edge is red-shifted with respect to ZnO, indicating that Zn in the sample may be higher than the +2 valence. Because the XAFS data are averaged, it is appropriate to state unequivocally that the sample Zn valence is near to +2. The Fourier converted X-ray absorption fine structure spectra of ZnO, Zn foil, and Zn-1.5TfOH/AC are shown in Fig. S5C. The curve of Zn-1.5TfOH/AC displays a high peak at 1.72 Å, which corresponds to the Zn−O bond. The sample's Zn−O peak position is greater than that of ZnO, indicating a longer Zn−O bond in the sample. The EXAFS fit curve of the extended edge data fits the experimental curve very well, as shown in Fig. 3, which is consisted with the results in the Table S3. The results of the experiment revealed that the primary support for the Zn element in the catalyst is Zn−O coordination, and the sample is a single-atom structure, and the fitted assessed Zn-O4 conformation by combining wavelet, k^3, and EXAFS data.

Based on the above analysis, the addition of TfOH would show a positive effect on the catalytic performance of Zn catalysts in the acetylene hydration, therefore, the catalytic performance of Zn-*x*TfOH/AC ($x = 0.5$, 1, 1.5, 2) catalysts was tested in the acetylene hydration reaction to investigate the effect of TfOH ligand on the performance of Zn/AC catalyst in acetylene hydration. Firstly, the effects of different temperatures on the performance of Zn-TfOH/AC catalysts in the acetylene hydration reaction were investigated as shown in Fig. S6 (Supporting information). It is clearly found that the catalytic activity of Zn-TfOH/AC an increasing trend with the increase of temperature, while the activity was reduced at the higher temperature of 260 °C, which indicated that the reaction temperature of 240 °C was better for the acetylene hydration. Furthermore, the effect of temperatures on the selectivity of acetaldehyde is more remarkable at the high reaction temperature.

Then, the catalytic performance of Zn-*x*TfOH/AC ($x = 0.5$, 1, 1.5, 2) catalysts was tested at the reaction temperature of 240 °C in the acetylene hydration reaction, and the results showed in Fig. 4. It can be seen that the Zn/AC catalyst has high initial activity but poor catalytic stability. However, with the increasing of TfOH ligand content, the catalytic activity was significantly enhanced and the stability was improved, especially for the Zn-1.5TfOH/AC catalyst with above 90% acetylene conversion and about 72% selectivity of acetaldehyde. Moreover, more addition of TfOH ligand content would cover the Zn active component species caused the reducing of the catalytic performance, which indicated that the optimal amount of addition was 1.5. The tested results confirmed that the introduction of TfOH ligand could show a significantly positive effect on the catalytic performance of Zn catalyst in the acetylene hydration.

For heterogeneous catalytic systems, the effect of catalyst dispersion on the catalyst performance is significant. Combined with the results of TEM, the Zn-*x*TfOH/AC ($x = 0.5$, 1, 1.5, 2) catalysts with the better dispersion of active species showed the better catalytic performance.

Lastly, in order to confirm the structure of the complex in the catalysts, the $Zn(OTf)_2$/AC catalyst was prepared with the same method and tested in the hydration of acetylene at the same reaction conditions. The catalytic activity results showed that $Zn(OTf)_2$/AC catalyst was almost inactive in the acetylene hydration. Combined with the results of XAFS characterization results, the Zn element in the catalyst is Zn−O coordination and the fitted assessed Zn-O4 conformation by combining wavelet, k^3, and EXAFS data, which confirmed that the Zn-1.5TfOH/AC with Zn−O coordination is more active for the acetylene hydration.

The TEM images of the fresh and used (Fig. S7 in Supporting information) catalysts showed that the addition of TfOH ligand could obviously promote the dispersion of Zn species on AC, reduce the agglomeration of Zn species particles during the reaction, and greatly improved the reaction activity. The loss rate of Zn species in the catalyst was characterized and analyzed by ICP-OES. The results are shown in Table S4 (Supporting information), the addition of TfOH significantly reduced Zn loss, and the amount of Zn loss gradually decreased as the content increased. When combined with the results of the XAFS analysis, it is hypothesized that the formation of coordination between Zn and the O atom in TfOH improves Zn interaction with the carrier and inhibits Zn loss. The ICP-OES and TEM characterization results are consistent with the activity test of the catalyst, which is consistent with the design of the initial experiment.

To further understand the chemical state and concentration of zinc, the fresh and used Zn-*x*TfOH/AC ($x = 0.5$, 1, 1.5, 2) catalysts were analyzed by XPS technique. Fig. 5 showed a blue shift in the binding energy of Zn $2p_{3/2}$ after the addition of the TfOH ligand, indicating that Zn lost electrons, lowering the electron cloud density around the active Zn species. This may be attributed to the strong electron-absorbing property of the S=O bond in trifluoromethanesulfonic [37], which also indicated the coordination interaction of Zn with TfOH. Furthermore, the magnitude of the blue shift in the binding energy of Zn $2p_{3/2}$ became more pronounced as the ligand quantity increased. The fitted curves of the Zn $2p_{3/2}$ peaks clearly show the fitted peaks corresponding to the chemical states of the two Zn species. The high binding energy is attributed to the $(ZnOH)^+$ species, while the low binding energy is attributed to the $(ZnH)^+$ species [19].

It has been speculated in the literature that Zn^{2+} with partial hydroxyl groups, *i.e.*, $(ZnOH)^+$ species, are produced on the surface of Zn catalysts after water vapor treatment [38]. Combined with the results of XPS analysis, the $(ZnOH)^+$ species in the Zn/AC catalyst was only 36.7%, so it is presumed that the $(ZnOH)^+$ species formed by the water vapor activation treatment is a small amount. In addition, related literature also shown that Zn^{2+} is capable of proton exchange with strongly acidic -OH groups, so we speculate that the B acid site may favor the formation of $(ZnOH)^+$ species [39,35]. In addition $(ZnOH)^+$ species are unstable and prone to dehydroxylation reactions in the presence of reducing gasses [38]. As shown in Table 1, the $(ZnOH)^+$ species in the catalyst gradually increased after the addition of TfOH ligand, and the $(ZnOH)^+$ species in the Zn-1.5TfOH/AC catalyst was 57.5%. Combined with the Py-FTIR characterization results, it appears that the addition of TfOH

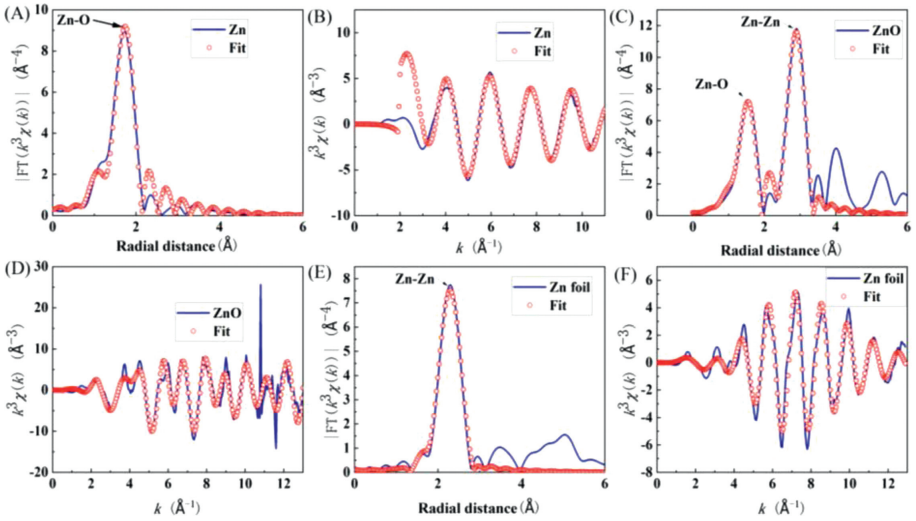

Fig. 3. Curves of Zn-fit-R (A), Zn-fit-k^3 (B), ZnO-fit-R (C), ZnO-fit-k^3 (D), Zn foil-fit-R (E) and Zn foil-fit-k^3 (F).

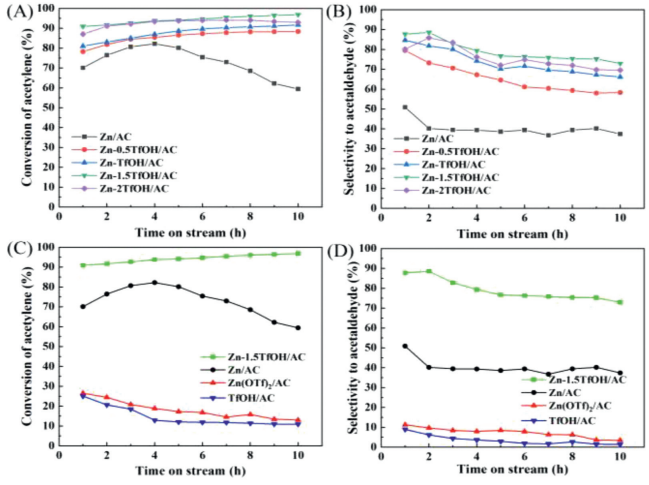

Fig. 4. Effect of Zn-xTfOH/AC catalysts (A, B), $Zn(OTf)_2$/AC and TfOH/AC catalyst (C, D) on the performance of acetylene hydration reaction.

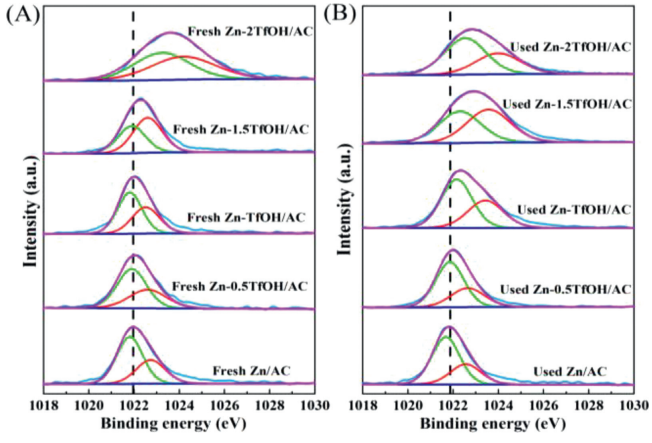

Fig. 5. Zn $2p_{3/2}$ XPS spectra of fresh catalysts (A) and used catalysts (B).

ligand increased the B-acid sites in the catalyst, which promoted the formation of $(ZnOH)^+$. In addition, since acetylene is a reducing gas, the $(ZnH)^+$ species are most likely formed by $(ZnOH)^+$ dehydroxylation. Py-FTIR analysis showed that the Zn-1.5TfOH/AC catalyst had the highest B acid content, while the Zn-1.5TfOH/AC catalyst had the largest percentage of $(ZnOH)^+$ species, which indicated that more $(ZnOH)^+$ species were more favorable for the reaction. The content of $(ZnOH)^+$ species in all catalysts was slightly reduced after the reaction compared to before the reaction, indicating that $(ZnOH)^+$ species were consumed during the reaction. This is also supported by the catalytic performance of the Zn-1.5TfOH/AC catalyst.

Table 1
Relative content of $(ZnH)^+$ and $(ZnOH)^+$ species on the catalyst surface.

Catalysts	Binding energy (eV)		Zn species content	
	$(ZnH)^+$	$(ZnOH)^+$	$(ZnOH)^+$	$(ZnH)^+$
Zn/AC	1021.8	1022.8	36.7%	63.3%
Used Zn/AC	1021.7	1022.6	32.4%	67.6%
Zn-0.5TfOH/AC	1021.9	1022.7	37.9%	62.1%
Used Zn-0.5TfOH/AC	1021.9	1022.7	35.4%	64.6%
Zn-TfOH/AC	1021.9	1022.6	41.9%	58.1%
Used Zn-TfOH/AC	1022.2	1022.5	39.8%	60.2%
Zn-1.5TfOH/AC	1021.9	1022.6	57.5%	42.5%
Used Zn-1.5TfOH/AC	1022.4	1023.6	52.1%	47.9%
Zn-2TfOH/AC	1023.3	1024.3	49.5%	50.5%
Used Zn-2TfOH/AC	1022.6	1024.1	45.4%	54.6%

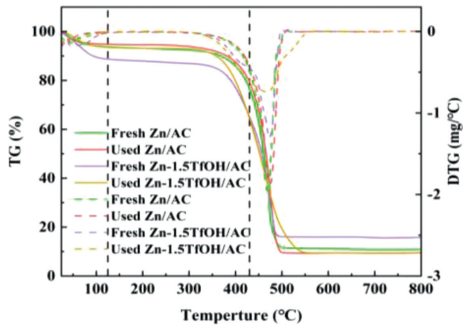

Fig. 6. TG and DTG curves of fresh and used catalysts.

According to the literature, carbon deposition is an important factor for the catalyst deactivation, in order to investigate the effect of TfOH ligand on the carbon deposition of Zn-based catalyst during the reaction, the Zn-xTfOH/AC ($x = 0.5$, 1, 1.5, 2) catalysts were analyzed with TG characterization, and the results are shown in Fig. 6 and Fig. S8 (Supporting information). Carbon depo-

Table 2
Carbon deposition of catalysts.

Catalysts	Amount of carbon deposition (%)
Zn/AC	2.96
Zn-0.5TfOH/AC	2.11
Zn-TfOH/AC	1.12
Zn-1.5TfOH/AC	1.19
Zn-2TfOH/AC	1.53

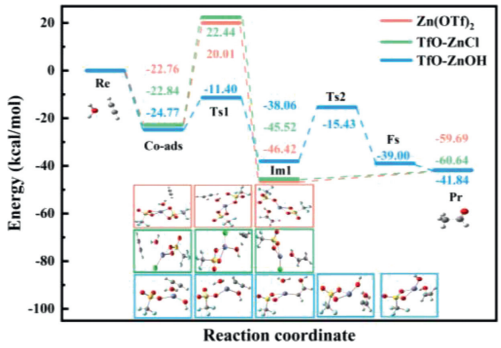

Fig. 7. Schematic energy profiles for the reaction pathway $Zn(OTf)_2$, TfO-ZnCl and TfO-ZnOH.

sition was calculated by estimating the weight difference between fresh and used catalysts in the same temperature range. The mass loss of the samples between room temperature and 130 °C was ascribed to the evaporation of water absorbed on the surface of the catalyst samples. The TG and DTG curves of fresh and used catalysts were basically identical, and both underwent $ZnCl_2$ breakdown and $(ZnOH)^+$ dehydroxylation between 350 °C and 600 °C. Table 2 showed that the carbon accumulation of the catalysts was significantly reduced after the addition of TfOH ligand, and the carbon accumulation of the Zn-1.5TfOH/AC catalyst was only 1.19%. These results demonstrated that Zn-1.5TfOH/AC is thermally stable and resistant to carbon buildup, which showed the excellent catalytic performance in the hydration of acetylene.

To further verify the catalytic active species in our prepared catalysts, the DFT simulation was employed in this part to explore the reaction pathway of different active species for acetylene hydration. According to the previous literature, three possible Zn coordinated species named $Zn(OTf)_2$, TfO-ZnOH, and TfO-ZnCl were investigated to obtain the adsorption energies and activation barriers. As shown in Fig. S9 (Supporting information), $Zn(OTf)_2$ is a tetracoordinate complex with the Zn atom combined with the four O atoms of the two (-OTf) perssad. For the three-coordinated TfO-ZnOH and TfO-ZnCl, the Zn atom was combined with two O atoms of one ligand and -OH(-Cl) group.

In order to explore which coordination structure is more favorable for acetylene hydration, as shown in Fig. 7, we speculated the reaction energy barriers of the three possible active ingredients, with TfO-ZnOH having a significantly lower reaction energy barrier than the other two coordination conformations. As established in the literature [24], for the initial step of Co-ads, all ligand configurations preferentially adsorb water before forming a Co-ads state because water has a greater adsorption energy than acetylene. The geometric configurations in the complete reaction pathway were displayed in Fig. 7, where a series of steps proceed from the co-adsorbed state (Co-ads) to the transition state (Ts) and then through several intermediates (Im) before forming the final product, acetaldehyde (Pr).

In exploring the reaction pathways, it was found that there is only one reaction pathway for each zinc coordination configuration. For the $Zn(OTf)_2$ structure, first it forms a Co-adsorbed state (Co-ads), then one of the O—H of the water molecule breaks and the dissociated OH^- adsorbs onto $Zn(OTf)_2$ to form the transition state Ts1. The process that requires overcoming the 42.77 kcal/mol energy barrier. Following that, H^+ and OH^- were combined with the two carbon atoms of acetylene to form an enol (Im1), which was then hydrolyzed to produce acetaldehyde (Pr represents the total energy of acetaldehyde and complexes) [31], while the active component reverted to the $Zn(OTf)_2$ structure. The pathway of the TfO-ZnCl structure is similar to that of $Zn(OTf)_2$. After forming the co-adsorbed state, when the dissociated OH^- adsorbs onto TfO-ZnCl to form the transition state Ts1, a process that requires overcoming the 45.28 kcal/mol energy barrier. Subsequently, H^+ and OH^- were added to the two carbon atoms of acetylene to form an enol (Im1), followed by the hydrolysis of Im1 to form acetaldehyde, while the active component reverts to the TfO-ZnCl structure.

Both $Zn(OTf)_2$ and TfO-ZnCl have only one transition state, Ts1, whereas TfO-ZnOH has two transition states, which differs from the previous two. The H_2O molecule does not dissociate after the formation of the co-adsorbed state (co-ads), the OH^- in TfO-ZnOH first undergoes an addition reaction with C_2H_2 to form Ts1, while the other carbon atom in acetylene reacts with Zn^{2+} in the catalyst interacts to form a vinyl metal complex to form the transition state Im1, while an energy barrier of 13.37 kcal/mol needs to be overcome. Then the O—H bond in the adsorbed water molecule breaks and the dissociated H^+ combines with the other carbon atom of acetylene to produce the vinyl alcohol Ts2, which undergoes a second transition state Ts2 with an energy barrier of 22.63 kcal/mol. Subsequently, a final state (Fs) of vinyl alcohol and TfO-ZnOH was formed, and finally, the adsorbed vinyl alcohol undergoes dissociation and hydrolysis to produce the target product acetaldehyde. Thus, the step that determines the rate is Ts2. The energy barrier of TfO-ZnOH is lower than that of $Zn(OTf)_2$ and TfO-ZnCl due to the presence of OH^- in the structure, which participates in the reaction and regenerates through the dissociation of H_2O molecules, lowering the energy barrier. Moreover, from a thermodynamic point of view, TfO-ZnOH is more favorable for the reaction due to the fact that Fs to Pr is an exothermic process. However, for the remaining two complex structures, the process is heat-absorbing.

In conjunction with the above study, TfO-ZnOH, which has the lowest energy barrier, is more likely to be the coordination structure of Zn and TfOH. Synchrotron radiation paired with XANES and EXAFS of the zinc K-edge revealed that Zn^{2+} developed a Zn-O4 coordination configuration during catalyst production. Because of the activation of high-temperature water vapor in the reaction phase, the Zn-O4 coordination conformation gradually opened, the Zn atom was combined with two O atoms of one ligand and -OH group. Consequently, forming TfO-ZnOH with a triple-ligand conformation could effectively increase reaction activity.

In this work, a series of Zn-TfOH/AC catalysts were synthesized, of which the Zn-1.5TfOH/AC catalyst showed the best catalytic performance in the hydration reaction of acetylene with 96% acetylene conversion. TEM and Py-FTIR characterization analysis showed that the addition of TfOH effectively promoted the dispersion of zinc species, while providing additional surface weak acid sites and catalytically active sites, which was favorable for the experiments. The XAFS test results showed that the element Zn was mainly present in the catalyst as a Zn—O coordination structure. The results of Py FTIR, XPS, ICP-OES and TG showed that TfOH ligand could increase the content of B acid and the relative content of $(ZnOH)^+$ species, enhance the interaction between zinc components and carriers, inhibit the loss of zinc species, and effectively enhance the stability of metal active species. The DFT calculations inferred that the TfO-ZnOH conformation is more likely to be a coordination structure formed by the zinc ligand, and the OH^- in TfO-ZnOH participates in the reaction and is regenerated by H_2O dissociation, thus re-

ducing the energy potential barrier. The above analysis is the main reason for the selective catalytic hydration of acetylene to acetaldehyde by Zn-1.5TfOH/AC catalyst.

Declaration of competing interest

We declare that we have no financial and personal relationships with other people of organizations that can inappropriately influence our work; there is no professional or other personal interest of any nature of kind in any product, service and/or company that could be construed as influencing the position presented in the manuscript entitled.

Acknowledgments

We gratefully acknowledge financial support provided by the High-level Talent Scientific Research Project of Shihezi University (Nos. RCZK201934 and SHYL-BQ201906) and the National Natural Science Funds of China (NSFC, No. 22178225).

Supplementary materials

Supplementary material associated with this article can be found, in the online version, at doi:10.1016/j.cclet.2022.107963.

References

[1] H.A. Wittcoff, J. Chem. Educ. 60 (1983) 1044–1047.
[2] A.S. Hester, K. Himmler, Ind. Eng. Chem. 51 (1959) 1424–1430.
[3] J. Smidt, W. Hafner, R. Jira, et al., Angew. Chem. 71 (1959) 176–182.
[4] R. Barthos, A. Hegyessy, G. Novodárszki, Z. Pászti, J. Valyon, Appl. Catal. A: Gen. 531 (2016) 96–105.
[5] D.A. Ponomarev, S.M. Shevchenko, J. Chem. Educ. 84 (2007) 1725–1726.
[6] I.T. Trotus, T. Zimmermann, F. Schuth, Chem. Rev. 114 (2014) 1761–1782.
[7] D.F. Othmer, K. Kon, T. Igarashi, Ind. Eng. Chem. 48 (1956) 1258–1262.
[8] W.L. Budde, R.E. Dessy, J. Am. Chem. Soc. 85 (1963) 3964–3970.
[9] K.K. Yee, Y.L. Wong, M. Zha, et al., Chem. Commun. 51 (2015) 10941–10944.
[10] G. Onyestyák, D. Kalló, Micropor. Mesopor. Mater. 61 (2003) 199–204.
[11] G. Onyestyák, G. Pal-Borbely, D. Kalló, Stud. Surf. Sci. Catal. 154 (2004) 2831–2838.
[12] J.M. Leslie, B.A. Tzeel, J. Chem. Educ. 93 (2016) 1100–1102.
[13] K. Nomiya, Y. Murara, Y. Iwasaki, et al., Mol. Catal. 469 (2019) 144–154.
[14] J. Halpern, B.R. James, A. Kemp, J. Am. Chem. Soc. 83 (1961) 4097–4098.
[15] M. Khan, S.B. Halligudi, S. Shukla, Z.A. Shaikh, J. Mol. Catal. 57 (1990) 301–305.
[16] L. Yang, F. Xiao, Q. Zhang, et al., ChemistrySelect 4 (2019) 7096–7101.
[17] A.J. Szonyi, W.F. Graydon, Can. J. Chem. Eng. 40 (1962) 183–187.
[18] R.B. Jain, Environ. Sci. Pollut. R 26 (2019) 30112–30118.
[19] Q.Q. Wang, M.Y. Zhu, H.Y. Zhang, et al., Catal. Lett. 3 (2018) 9603–9609.
[20] Q. Wang, M. Zhu, B. Dai, J. Zhang, Chin. Chem. Lett. 30 (2019) 1244–1248.
[21] Q.Q. Wang, M.Y. Zhu, H.Y. Zhang, et al., Catal. Commun. 120 (2019) 33–37.
[22] Q.Q. Wang, M.Y. Zhu, C.X. Xu, et al., New J. Chem. 42 (2018) 6507–6514.
[23] Q.Q. Wang, M.Y. Zhu, B. Dai, J.L. Zhang, Catal. Sci. Technol. 9 (2019) 981–991.
[24] J.Q. Li, Y. Zhao, M.Y. Zhu, L.H. Kang, J. Mol. Model. 26 (2020) 105.
[25] J.Q. Li, L.H. Kang, Mater. Today Commun. 27 (2021) 102216.
[26] L. Yang, H.W. Chen, R.C. Su, C.X. Xu, B. Dai, Catal. Lett. 148 (2018) 3370–3377.
[27] Q. Zhang, X.H. Liu, J.N. Luo, C.H. Ma, C.X. Xu, New J. Chem. 45 (2021) 1712–1720.
[28] Q. Zhang, X.J. Chen, Y. Xie, et al., Int. J. Hydrog. Energy 47 (2022) 8238–8246.
[29] X.H. Liu, X.J. Chen, Q. Zhang, C.X. Xu, Mol. Catal. 522 (2022) 112223.
[30] Y.F. Liu, R.Z. Liao, W.J. Ding, J.G. Yu, R.Z. Liu, J. Biol. Inorg. Chem. 16 (2011) 745–752.
[31] A. Najafian, T.R. Cundari, Polyhedron 154 (2018) 114–122.
[32] M. Nishizawa, M. Skwarczynski, H. Imagawa, T. Sugihara, Chem. Lett. 31 (2002) 12–13.
[33] R.E. Ebule, D. Malhotra, G.B. Hammond, B. Xu, Adv. Synth. Catal. 358 (2016) 1478–1481.
[34] T.W. Bai, X.F. Ni, J. Ling, Z.Q. Shen, Chin. J. Polym. Sci. 37 (2019) 990–994.
[35] X.J. Niu, J. Gao, Q. Miao, et al., Micropor. Mesopor. Mater. 197 (2014) 252–261.
[36] E. Modrogan, M.H. Valkenberg, W.F. Hoelderich, J. Catal. 261 (2009) 177–187.
[37] A. Orita, J. Xiang, K. Sakamoto, J. Otera, J. Organomet. Chem. 624 (2001) 287–293.
[38] S. Tamiyakul, T. Sooknoi, L.L. Lobban, S. Jongpatiwut, J. Appl. Catal. A: Gen. 525 (2016) 190–196.
[39] L.A.M.M. Barbosa, R.A.V. Santen, Catal. Lett. 63 (1999) 97–106.